Similarity Solutions for the Converging or Diverging Steady Flow of Non-Newtonian Elastic Power Law Fluids with Wall Suction or Injection

Part I: Two-Dimensional Channel Flow

R. T. BALMER and JAMES J. KAUZLARICH

University of Virginia, Charlottesville, Virginia

Similarity solutions are determined for the steady flow of an incompressible elastic power law fluid in a two-dimensional channel with nonparallel walls. The possibility of wall suction or injection is considered. Solutions are found to exist only for power law indices of unity. A method is developed for estimating the pressure drop in the naturally converging flow field before the entrance to a capillary. In diverging flows a singularity is found to arise due to the elasticity of the fluid. The singularity corresponds to a Deborah number of unity. It is postulated that the singularity is, for the constitutive equation used here, a possible source of the flow instability commonly referred to as melt fracture.

The equations of motion of a Newtonian fluid in various converging-diverging geometries have been treated successfully by several authors. Blasius (*14*) investigated diverging flows of incompressible fluids through consideration of the entire momentum equations. Jeffery (*24*) and Hamel (*20*) solved the complete momentum equations in polar coordinates for converging-diverging flow of an incompressible fluid between plane walls. Rosenhead (*38*) and later Millsaps and Pohlhausen (*33*) produced numerical values for Jeffery and Hamel's results. Earlier, Pohlhausen (*37*) developed a similarity solution for the boundary-layer equations applied to the convergent flow of an incompressible fluid between plane walls. Berman (*10*, *11*), Sellars (*42*), and Yuan (*58*) investigated the steady two-dimensional incompressible viscous Newtonian flow in a channel with wall suction using the complete momentum equations. More recently, Williams (*56*, *57*) constructed a similarity solution for the boundary-layer equations applied to the convergent or divergent flow of a compressible or incompressible fluid in a channel with a variable wall profile. Smith (*45*) extended Williams' analysis of incompressible flows to include wall suction or injection. This paper extends Smith's analysis of two-dimensional channel flows by introducing an incompressible non-Newtonian fluid with elastic properties.

SIMILARITY TECHNIQUE

The similarity technique is an analytical method for solving partial differential equations. It involves discovering a transformation of variables that will reduce the number of independent variables, thus ultimately producing an ordinary differential equation which can be either analytically or numerically solved (*21*).

The two-dimensional momentum equations for incompressible steady flow are (*40*)

$$\rho\left(u^*\frac{\partial u^*}{\partial x^*}+v^*\frac{\partial u^*}{\partial y^*}\right)=-\frac{\partial p^*}{\partial x^*}+\frac{\partial T^*_{xx}}{\partial x^*}+\frac{\partial T^*_{xy}}{\partial y^*}$$
$$\rho\left(u^*\frac{\partial v^*}{\partial x^*}+v^*\frac{\partial v^*}{\partial y^*}\right)=-\frac{\partial p^*}{\partial y^*}+\frac{\partial T^*_{yy}}{\partial y^*}+\frac{\partial T^*_{xy}}{\partial x^*} \quad (1)$$

where the asterisks indicate that the quantities are dimensional, and T^*_{ij} is the ij^{th} physical component of the deviatoric stress tensor $[\mathbf{T}^*]$. Equations (1) can be nondimensionalized by introducing the following quantities:

$$u=u^*/U \qquad [\mathbf{T}]=(1/\rho U^2)\cdot[\mathbf{T}^*]$$
$$v=v^*/U \qquad x=x^*/L \quad (2)$$
$$p=p^*/\rho U^2 \qquad y=y^*/L$$

The origin of the coordinate system is on the channel center line (see Figure 9).

Substitution of (2) into (1) gives the nondimensional momentum equations:

$$u\frac{\partial u}{\partial x}+v\frac{\partial u}{\partial y}=-\frac{\partial p}{\partial x}+\frac{\partial T_{xx}}{\partial x}+\frac{\partial T_{xy}}{\partial y}$$
$$u\frac{\partial v}{\partial x}+v\frac{\partial v}{\partial y}=-\frac{\partial p}{\partial y}+\frac{\partial T_{yy}}{\partial y}+\frac{\partial T_{xy}}{\partial x} \quad (3)$$

Equations (3) can be simplified somewhat by an order of magnitude analysis. We require at the outset that the injection or suction be kept small, such that $v^* \ll U$. Now, the characteristic axial velocity is of the same order of magnitude as the axial velocity, so

$$u=0(1)$$

Since the flow is incompressible, the wall profile smooth, and the injection small, it is reasonable to take (*45*)

$$\partial u/\partial x=0(1)$$

From the continuity equation it follows that

$$\frac{\partial v}{\partial y}=0\left(\frac{\partial u}{\partial x}\right)=0(1)$$

R. T. Balmer is at the University of Wisconsin, Milwaukee, Wisconsin.

Thus we will take

$$x = 0(1) \quad \text{and} \quad y = 0(\delta)$$

where $\delta \ll 1$.

Now,

$$u = 0(1) \quad \text{and} \quad v = 0(\delta)$$

$$u\frac{\partial u}{\partial x} = 0(1) \qquad v\frac{\partial v}{\partial y} = 0(\delta)$$

$$v\frac{\partial u}{\partial y} = 0(1) \qquad u\frac{\partial v}{\partial x} = 0(\delta)$$

Terms of order δ neglected, Equation (3) becomes

$$u\frac{\partial u}{\partial x} + v\frac{\partial u}{\partial y} = -\frac{\partial p}{\partial x} + \frac{\partial T_{xx}}{\partial x} + \frac{\partial T_{xy}}{\partial y} \tag{4a}$$

$$0 = -\frac{\partial p}{\partial y} + \frac{\partial T_{yy}}{\partial y} + \frac{\partial T_{xy}}{\partial x} \tag{4b}$$

Integrating Equation (4b) gives

$$p(x,y) = T_{yy}(x,y) + \int_0^y \frac{\partial T_{xy}}{\partial x}\,dy + p(x,0) - T_{yy}(x,0)$$

Differentiating this with respect to x and substituting it into Equation (4a) gives

$$u\frac{\partial u}{\partial x} + v\frac{\partial u}{\partial y} = \frac{\partial}{\partial x}(T_{xx} - T_{yy}) + \frac{\partial T_{xy}}{\partial y} - \int_0^y \frac{\partial^2 T_{xy}}{\partial x^2}\,dy + f(x), \tag{5}$$

where

$$f(x) = -\frac{\partial}{\partial x}[p(x,0) - T_{yy}(x,0)]$$

CONSTITUTIVE EQUATION

The constitutive equation chosen for this work is valuable because of its apparent ability to be easily fit to experimental data over significant shear rate regions. Power law fluids of various types have been used with great success in the study of similarity solutions of external boundary-layer flows (*1, 13, 16, 17, 19, 22, 25, 41*). The formal constitutive equation used here is very similar to the one used by Metzner and White (*30*) and Uebler (*51*). The deviatoric stress matrix in dimensional form is

$$[\tilde{\mathbf{T}}^*] = \begin{bmatrix} \frac{1}{2}\xi\left(\frac{\partial u^*}{\partial y^*}\right)^s & \mu\left(\frac{\partial u^*}{\partial y^*}\right)^n & 0 \\ \mu\left(\frac{\partial u^*}{\partial y^*}\right)^n & -\frac{1}{2}\xi\left(\frac{\partial u^*}{\partial y^*}\right)^s & 0 \\ 0 & 0 & -\frac{1}{2}\xi\left(\frac{\partial u^*}{\partial y^*}\right)^s \end{bmatrix} \tag{6}$$

Note that in (6) the Weissenberg hypothesis (*52*) regarding the normal stresses in the directions perpendicular to the flow direction is assumed to be valid, although it was not necessary to have done so.

In Equation (6), ξ and s are, respectively, the normal stress coefficient and the normal stress power law exponent; and μ and n are, respectively, the apparent viscosity and shear stress power law exponent. All of these are assumed constant over an appropriate shear rate range.

Consider the first and third terms on the right-hand side of Equation (5). In dimensionless form Equation (6) gives

$$T_{xx} - T_{yy} = \frac{1}{N}\left(\frac{\partial u}{\partial y}\right)^s$$

and

$$T_{xy} = \frac{1}{N_{Re}}\left(\frac{\partial u}{\partial y}\right)^n$$

where

$$N = \frac{\rho U^{2-s} L^s}{\xi} = \text{power law Reynolds number in } s$$

and

$$N_{Re} = \frac{\rho U^{2-n} L^n}{\mu} = \text{power law Reynolds number in } n$$

Now, the terms of Equation (5) in question are

$$\frac{\partial}{\partial x}(T_{xx} - T_{yy}) - \frac{\partial}{\partial x}\int_0^y \frac{\partial T_{xy}}{\partial x}\,dy$$

$$= \frac{\partial}{\partial x}\int_0^y \left[\frac{\partial}{\partial y}(T_{xx} - T_{yy}) - \frac{\partial T_{xy}}{\partial x}\right]dy$$

$$= \frac{\partial}{\partial x}\int_0^y \left[\frac{s}{N}\left(\frac{\partial u}{\partial y}\right)^{s-1}\frac{\partial^2 u}{\partial y^2} - \frac{n}{N_{Re}}\left(\frac{\partial u}{\partial y}\right)^{n-1}\frac{\partial^2 u}{\partial y\,\partial x}\right]dy$$

Also

$$\left(\frac{\partial u}{\partial y}\right)^{s-1}\frac{\partial^2 u}{\partial y^2} = 0\left(\frac{1}{\delta^{s+1}}\right)$$

and

$$\left(\frac{\partial u}{\partial y}\right)^{n-1}\frac{\partial^2 u}{\partial y\,\partial x} = 0\left(\frac{1}{\delta^n}\right)$$

Inspection of data taken for various materials yields the result that usually $s \geq n$ (*30*). Thus the later expression is at least one order of magnitude less than the former.

Henceforth, the term $\int_0^y \frac{\partial T_{xy}}{\partial x}\,dy$ will be neglected in comparison with the term $T_{xx} - T_{yy}$.

Application of Equation (6) to Equation (5) produces

$$u\frac{\partial u}{\partial x} + v\frac{\partial u}{\partial y} = \frac{1}{N_{Re}}\left[\frac{\partial}{\partial y}\left(\frac{\partial u}{\partial y}\right)^n\right] + \frac{1}{N}\left[\frac{\partial}{\partial x}\left(\frac{\partial u}{\partial y}\right)^s\right] + f(x) \tag{7}$$

If the stream function Ψ is defined with the equations

$$u = \frac{\partial \Psi}{\partial y} = \Psi_y$$

$$v = -\frac{\partial \Psi}{\partial x} = -\Psi_x$$

then the continuity equation is automatically satisfied and Equation (7) becomes

$$\Psi_y\Psi_{xy} - \Psi_x\Psi_{yy} = \frac{1}{N_{Re}}[n(\Psi_{yy})^{n-1}\Psi_{yyy}] + \frac{1}{N}[s(\Psi_{yy})^{s-1}\Psi_{yyx}] + f(x) \tag{8}$$

A similarity transformation is assumed of the form

$$\Psi = g(x)F(\eta) \tag{9}$$

where $\eta = y/R(x)$, and $R(x)$ and $g(x)$ are the channel wall profile and injection (or suction) parameters, respectively.

Substitution of Equation (9) into Equation (8) produces

$$nF''' - N_{Re}\left(\frac{gF''}{R^2}\right)^{1-n}\left[R^2\frac{d}{dx}\left(\frac{g}{R}\right)(F')^2 - R\frac{dg}{dx}FF'' - \frac{R^3}{g}f(x)\right] = s\left(\frac{gF''}{R^2}\right)^{s-n}(N_{WS}) \times\left[\frac{dR}{dx}F''' - \frac{R^3}{g}\frac{d}{dx}\left(\frac{g}{R^2}\right)F''\right] \quad (10)$$

where $N_{WS} = N_{Re}/N$ = Weissenberg number (the ratio of elastic to viscous forces). In order that Equation (10) be an ordinary differential equation, R and g must satisfy the following set of conditions (*21*):

a. $(g/R^2)^{1-n} = C_1$

b. $R^2\frac{d}{dx}(g/R) = C_2$

c. $R\frac{dg}{dx} = C_3$

d. $(g/R^2)^{s-n} = C_4$ (11)

e. $\frac{dR}{dx} = C_5$

f. $(R^3/g)\frac{d}{dx}\left(\frac{g}{R^2}\right) = C_6$

g. $(R^3/g)f(x) = C_7$

where C_1 through C_7 are all constants. Combination of conditions e, c, and b or f reveals that g must be a constant and that R can be at most linear in x. That is, the walls must be plane converging or diverging and there can be no suction or injection at the walls.† Conditions a, d, and f are satisfied for any values of s and n if both $R(x)$ and $g(x)$ are taken to be constant. Note that under these latter conditions Equation (10) reduces to an equation which is independent of s or N_{WS} and hence is independent of the fluid elasticity. Channel flow between infinite parallel walls is steady in the Lagrangian sense and consequently has a zero Deborah number. Hence it is not surprising to find that under these conditions Equation (9) is devoid of all elasticity parameters.‡

The only other case of interest is when $s = n = 1$. The conditions of $n = 1$ implies that the fluid is being sheared near its lower or possibly its upper (*12*) Newtonian region. The implications of setting $s = 1$ are less clear. Experiments tend to indicate that near the lower Newtonian region the normal stress difference is proportional to the square of the shear rate (that is, $s = 2$) (*31*). However it has not been demonstrated that all non-Newtonian fluids must necessarily behave in this matter. Thus maintaining $s = 1$ in this analysis appears to be a sufficiently accurate condition to at least approximate real fluid behavior.

Thus in order to transform Equation (10) into an ordinary differential equation nontrivially, the following conditions are required to be valid:

$$R = k_1x + k_2$$
$$g = k_3 \quad (12)$$
$$n = s = 1$$

†It is worth noting here that the axisymmetric converging or diverging flow problem for the same constitutive equation also requires straight walls, but does not allow suction or injection at the wall (*8*). This will be discussed in Part II of this series.

‡This does not mean that there are no normal stresses in this type of flow, for inspection of Equation (6) reveals that they certainly exist here. It simply means that the normal stresses that do exist have no influence on the velocity profiles. This fact has been noted by Seyer and Metzner (*43*). However the normal stresses do have an influence when the walls are nonparallel.

When $n = s = 1$ and $N_{WS} = 0$, then Equation (10) reduces to Smith's (*45*) equation for an incompressible Newtonian fluid in converging or diverging two-dimensional channel flow. The boundary conditions on Equation (10) are

$$F(0) = 0 \quad (13a)$$
$$F'(1) = 0 \quad (13b)$$
$$F''(0) = 0 \quad (13c)$$

where condition (13a) arbitrarily assigns the value of zero to the stream function corresponding to the channel center line ($y = 0$) (*45*), condition (13b) is the no slip condition at the wall ($y = R$), and condition (13c) is the condition of flow symmetry about the channel center line.

NUMERICAL RESULTS

Utilization of Equations (12) reduces Equation (10) to

$$(1 - N_{WS}k_1\eta)H''' - 2N_{WS}k_1H'' + N_{Re}k_1k_3\alpha(H')^2 = 1 \quad (14)$$

where $H = F/\alpha$ and

$$\alpha = -\frac{N_{Re}R^3}{g}f(x)$$

The numerical solution of Equation (14) subject to the boundary conditions (13) is shown in Figures 1 through 4 for a 10-deg. converging channel and Figures 5 through 8 for a 10-deg. diverging channel. This channel angle was chosen to correspond to that used by Williams (*56*, *57*) and Millsaps and Pohlhausen (*33*). The definition of Reynolds number used here is the same as that used by others (*33*, *45*, *56*, *57*):

$$N_{Re} = \frac{UL}{\nu} = \frac{1}{\nu}(u_{\mathbb{C}})\frac{R}{\tan\theta} = \frac{g\alpha H'(0)}{\nu\tan\theta} \quad (15)$$

where θ is the wall half-angle.

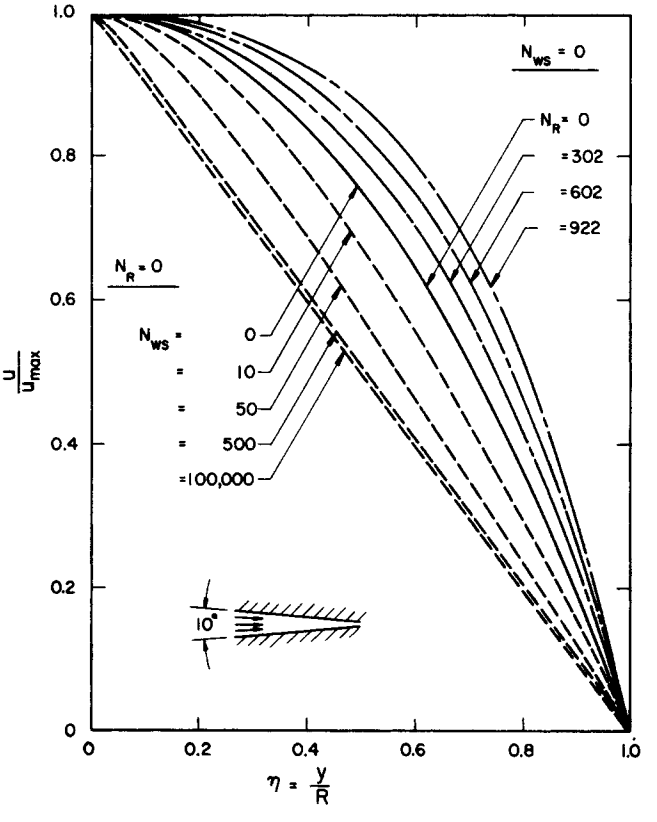

Fig. 1. Axial velocity profiles in a 10-deg. convergent channel for independently viscous and elastic fluids.

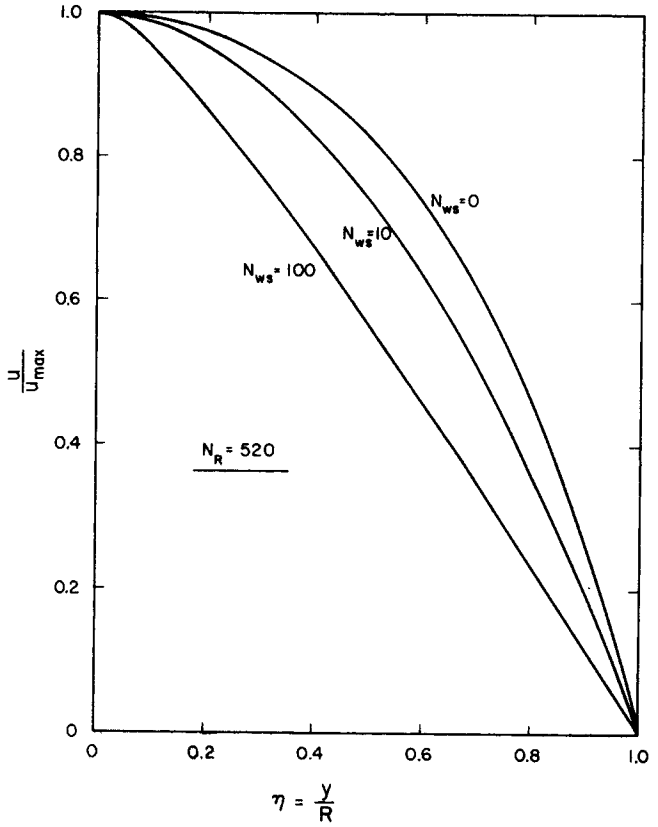

Fig. 2. Axial velocity profiles in a 10-deg. convergent channel illustrating the effect of fluid elasticity on a viscous flow ($N_R = 520$).

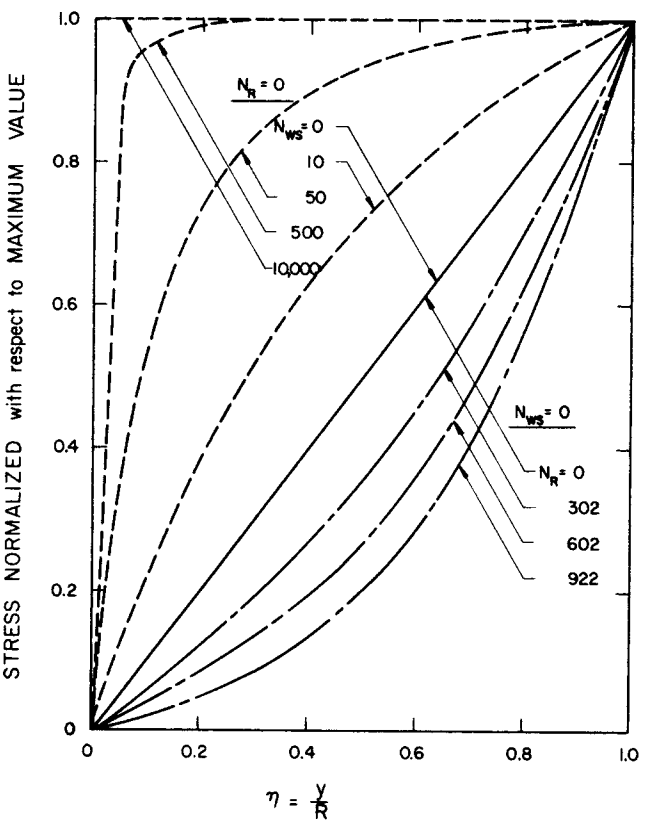

Fig. 4. Normalized stress distributions in a 10-deg. convergent channel for independently viscous and elastic fluids.

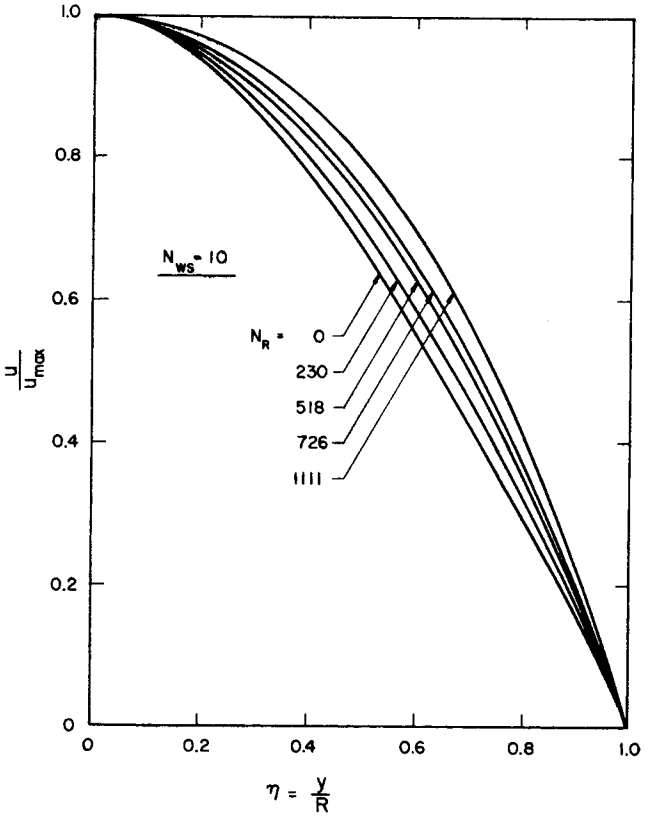

Fig. 3. Axial velocity profiles in a 10-deg. convergent channel illustrating the effect of fluid viscosity on an elastic flow ($N_{WS} = 10$).

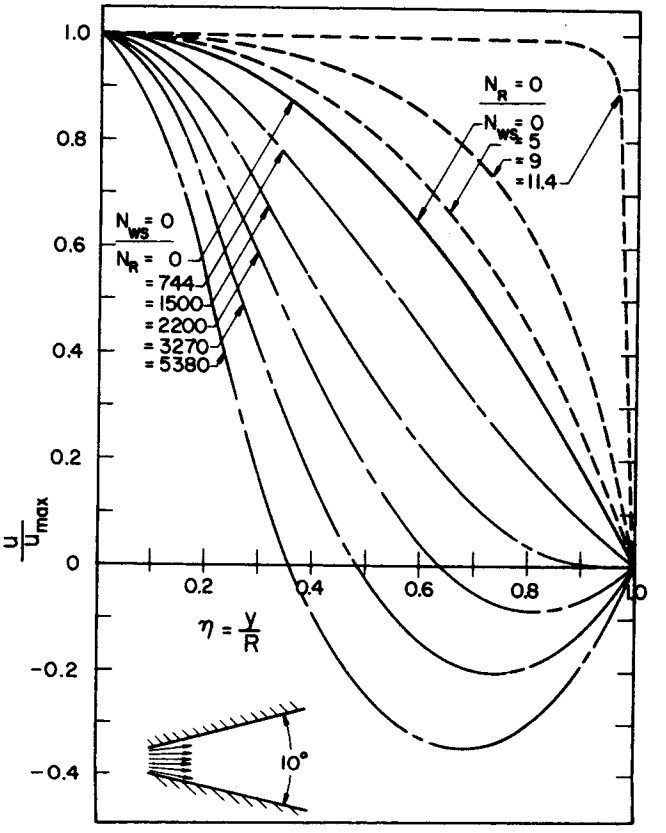

Fig. 5. Axial velocity profiles in a 10-deg. divergent channel for independently viscous and elastic fluids.

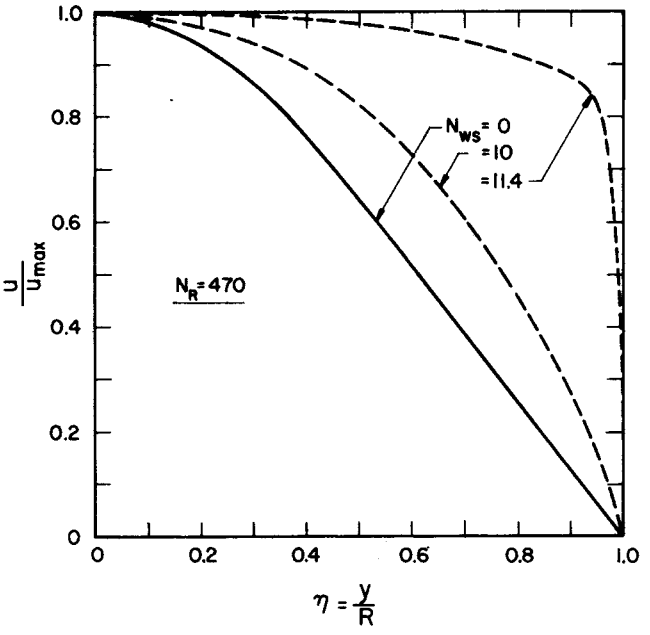

Fig. 6. Axial velocity profiles in a 10-deg. divergent channel illustrating the effect of fluid elasticity on a viscous flow (N_R = 470).

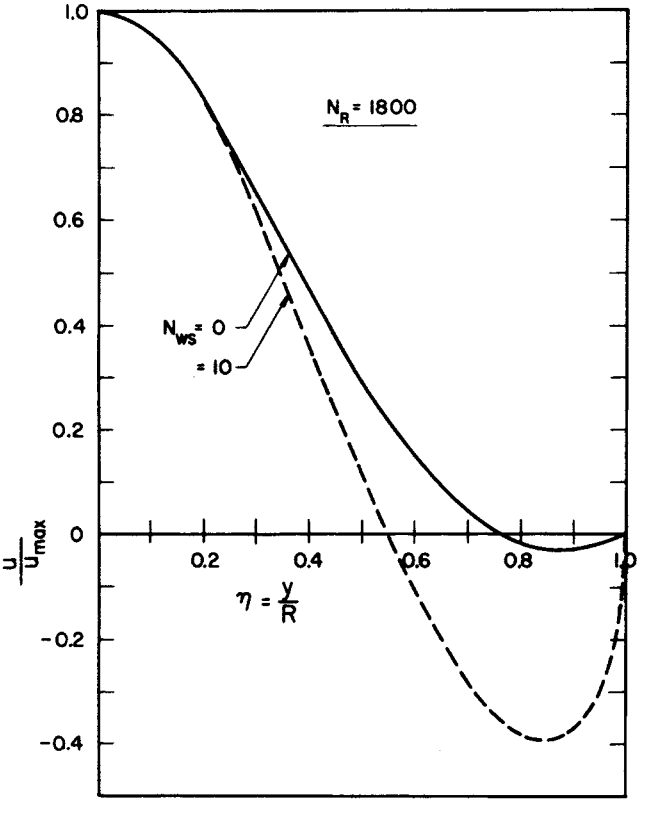

Fig. 7. Axial velocity profiles in a 10-deg. divergent channel illustrating the effect of fluid elasticity on a viscous flow (N_R = 1,800).

When $N_{Re} = 0$, Equation (14) can be solved analytically to yield the elastic liquid result:

$$H(\eta) = -\frac{\log_e (1 - N_{WS}k_1\eta)}{2N_{WS}^3k_1^3} - \frac{\eta^2}{4N_{WS}k_1} + \frac{\eta}{2N_{WS}k_1}\left[1 - \frac{1}{N_{WS}k_1(1 - N_{WS}k_1)}\right] \quad (16)$$

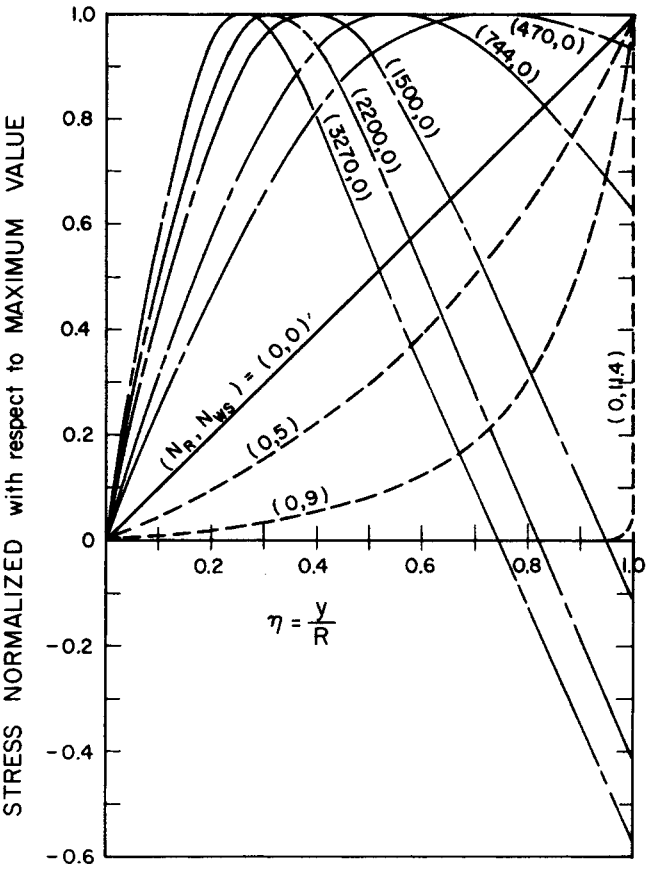

Fig. 8. Normalized stress distributions in a 10-deg. diverging channel for independently viscous and elastic fluids.

These elastic liquid flows are shown in Figures 1, 4, 5, and 8 ($N_R = 0$, $N_{WS} \neq 0$).

DISCUSSION OF RESULTS

Hansen and Na (*35*) have shown that the only similarity solutions of the boundary-layer equations for a reasonably general non-Newtonian fluid in external flow that can exist are for flows over a wedge. White and Metzner (*55*) arrive at the same conclusion using a considerably less general constitutive equation. The similarity solution presented here complies with Hansen's criterion in that it is a form of internal wedge type flow.

In converging flow Figures 1 and 2 indicate that the effect of fluid elasticity is to produce a more pointed velocity profile than normal. Figure 4 indicates that elasticity tends to broaden the stress distribution in this type of flow. Furthermore from comparison of Figures 1 and 3, it takes a Reynolds number of roughly 70 times the value of the Weissenberg number to counterbalance the effect of the Weissenberg number. Consequently, a small amount of elasticity can have a large effect in this type of flow.

In diverging flow the effect of fluid elasticity is quite different. Figures 5, 6, and 8 indicate that for low Reynolds numbers, elasticity tends to broaden the velocity distribution and thus reduce the stress distribution. However Figure 7 indicates that when backflow occurs fluid elasticity has the curious effect of increasing the backflow near the walls, but at the same time leaving the velocity distribution near the center line relatively unchanged. If this is in fact true, then, in this type of flow field, fluid elasticity would seem to precipitate early flow separation rather than enhance flow stability. However, many authors (*23, 39*) suggest that fluid elasticity tends to damp turbulent fluc-

tuations and thus promote laminar stability. The effect of fluid elasticity on velocity profile trends as observed here is remarkably similar to that reported by Mishra and Roy (*34*) in studying the flow of an elasticoviscous liquid between rotating cylinders.

This analysis also produced solutions in which the velocity profile had more than one maximum and minimum. These types of solutions were investigated earlier by Rosenhead (*38*) and Williams (*57*). However, as pointed out by Rosenhead, the lack of experimental verification of these flow fields casts some doubt on their stability. For this reason they will not be considered further here.

DEBORAH AND WEISSENBERG NUMBERS

The Deborah number is taken here to be (*44*)

$$N_{Deb} = \lambda / t_p \tag{17}$$

A constitutive equation defines the character of a fluid. However the constitutive equation used here [Equation (6)] does not define a characteristic time for this fluid. Thus we are free to complete the fluid characterization by arbitrarily defining its characteristic time. The characteristic time is taken such that the Weissenberg number used in the development of Equation (10) becomes identical to the more general definition used by Slattery (*44*), that is

$$N_{WS} = \frac{\xi}{\mu}\left(\frac{L}{U}\right)^{n-s} = \frac{\lambda U}{L} \tag{18}$$

Thus

$$\lambda = \frac{\xi}{\mu}\left(\frac{L}{U}\right)^{n-s+1} \tag{19}$$

In Equation (17) the process time t_p is typically taken as L/U. Astarita suggests (*3*, *4*) that the characteristic length L for the process-dependent Deborah number be taken in the direction of flow and that the characteristic length for the shear-dependent Weissenberg number be taken normal to the direction of flow. In general these two lengths are unequal and thus the Deborah and Weissenberg numbers are unequal. On the other hand, Slattery (*44*) contends that when t_p, U and L are related (as they are here), then $N_{WS} = N_{Deb}$, and therefore there is only one significant characteristic length. Clearly these two authors are at odds with each other. In this paper Astarita's interpretation has been chosen for reasons that will become apparent later.

In the flow field considered here one can associate with each point two characteristic lengths and one characteristic velocity. The characteristic length L_1 is taken as the distance measured along the axis from an arbitrary point to the channel apex. L_2 is the distance measured normal to the channel axis (at the same point which defines L_1) to the channel wall. These lengths are related as

$$\frac{L_2}{L_1} = \tan\theta \tag{20}$$

The characteristic velocity is taken to be the corresponding center line velocity. Thus the Deborah and Weissenberg numbers become

$$N_{Deb} = \frac{\lambda u_{\mathbb{C}}}{L_1}, \quad N_{WS} = \frac{\lambda u_{\mathbb{C}}}{L_2} \tag{21}$$

and are related as

$$N_{Deb} = N_{WS}(\tan\theta) \tag{22}$$

Inspection of Equation (14) reveals a singularity in the first term. Thus the Weissenberg number cannot exceed the critical value given by

$$(N_{WS})_{crit} = \frac{1}{k_1} = \frac{1}{\tan\theta} \tag{23}$$

From Equation (22) the critical Deborah number becomes

$$(N_{Deb})_{crit} = 1 \tag{24}$$

Several intuitive arguments have been set forth establishing the critical Deborah number at unity for all flow geometries (*2*, *27*, *29*). However, to the authors' knowledge, Equation (24) represents the only instance wherein the condition of unit critical Deborah number has been derived directly from the equations of motion. This was the primary reason for adopting Astarita's interpretation of the characteristic lengths. Had Slattery's position been accepted, then it would have been necessary to admit that the value of the Deborah number at which the equations of motion broke down was much greater than unity, and this would be contrary to the published results of others (*2*, *27*, *29*, *54*).

Note that as θ goes to zero (infinitely long parallel plates), neither the Weissenberg nor the Deborah number places any limitation on the flow field. Furthermore unlike the Deborah number, there is no numerical upper limit for the critical Weissenberg number.

Use of Equation (12) with $k_2 = 0$ gives the critical length from the apex of the channel in which fluid elasticity becomes dominant as

$$x_{crit} = \left[\frac{\lambda k_3 \alpha H'(0)}{\tan\theta}\right]^{1/2} \tag{25}$$

This means, for example, that in a configuration such as Figure 9 there would be solidlike elastic behavior in the region shown shaded. This presupposes that if one attempts to exceed the values of the critical elastic numbers, the material behaves totally elastically as predicted by several authors (*2*, *5*, *27*, *29*, *30*, *54*).

MELT FRACTURE

The dramatic phenomenon of melt fracture, or elastic turlence, (*26*, *32*) has thus far remained kinematically unsolved. There are at least four explanations of this unusual flow field in the current literature: the capillary exit effect (*46*), the capillary entrance effect (*7*, *15*, *48*, *49*, *50*), a purely hydrodynamical effect inside the capillary (*36*), and a stick-slip mechanism which also occurs exclusively inside the capillary (*9*, *47*). White (*53*), through analysis of the dimensionless groups which arise from the equations of motion, has concluded that melt fracture should occur at a critical value of the Weissenberg number. Pearson and Petrie (*36*) also conjecture that melt fracture is directly related to fluid elasticity.

The phenomenon of melt fracture may be at least partially explained by the results of this analysis. Equation (14), if interpreted as an elementary description of the instability

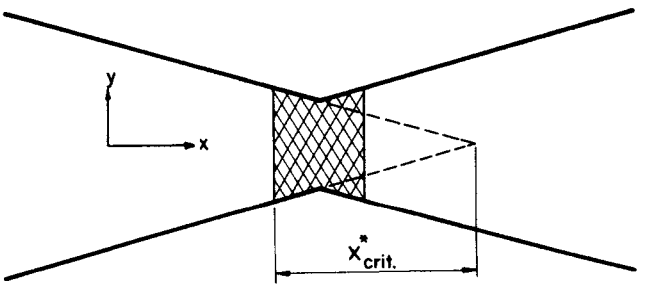

Fig. 9. Illustration of critical length defining elastic solidlike behavior, based on a Deborah number of unity.

resulting in the solidlike elastic behavior of melt fracture, is seen to comply exactly with White's conjecture. Thus it may be that the requirements for melt fracture to occur are twofold. First, the fluid is required to exhibit elastic properties ($N_{WS} \neq 0$), and second it is required that the flow field contain a small region of diverging flow.

If at the entrance to a capillary tube a vena contracta existed, then the flow field would contain a region of diverging flow. If there is diverging flow, then solidlike elastic behavior could manifest itself in the manner described above. Unfortunately, very little is currently known about the entrance vena contracta of non-Newtonian fluids. Apparently, in recent times very few experimenters have been concerned with this facet of the flow field. Only Drexler's recent work (*18*) directly indicates the possibility of a vena contracta in certain non-Newtonian entrance flows. However, experimentally, we find that melt fracture does not exist at all shear (flow) rates, but it only exists for shear rates above a certain value (the value depending upon the fluid, the geometry, etc.). In Newtonian fluids the entrance vena contracta is known to exist only at the higher shear rates; therefore the same may be true of the entrance vena contracta in non-Newtonian fluids, if it exists in general. Consequently it may be concluded that the existence of a vena contracta (with its associated diverging flow field) at the entrance to a capillary is, under the proper conditions, sufficient to theoretically produce solidlike elastic material behavior as described by Equations (23) and (24).

Requiring a vena contracta as the source of all melt fracture essentially limits this phenomenon to be of the capillary entrance type. There have been several photographic studies by Tordella (*48* to *50*), Clegg (*15*), and Bagley (*7*) that indicate that this is in fact true. However there is also equally good evidence by Benbow (*9*) and Tordella (*47*) that indicates that the flow instability does not necessarily need an entrance to precipitate itself. In fact, Tordella (*47*) suggests the existence of two types of melt fracture, "inlet fracture" and "land fracture." While a vena contracta appears to be a sufficient condition to initiate solidlike behavior, it is not a necessary requirement. There may be other much more subtle flow phenomena (such as boundary-layer effects or molecular fractionation) that could produce a locally diverging flow field. Presumably, these later phenomena could occur above the entrance to the capillary or even inside the capillary itself.

Careful inspection of the photographs of particle paths by Tordella (*49*), Clegg (*15*), and Bagley (*7*) reveals what in certain cases appears to be a slightly diverging flow just above the capillary entrance [for example, see Bagley's Figures 4, 5, and 6 (*7*)]. A converging section or, as Bagley notes, a "wine glass stem funnel," is formed at the entrance to the capillary at low flow rates. As the flow rate is increased the regions of backflow seem to pinch off the converging stem right above the capillary entrance, thus forming a small converging-diverging region. Decreasing the capillary inlet angle has been known for some time to produce a more stable flow. In view of the results presented here these effects could be due simply to the associated reduction in the size of the backflow region and thus a reduction in the effect this region has on the main flow.

It should be noted that once the flow fluctuations have begun, then there will always be sufficient diverging flow regions to perpetuate the instability so long as the Weissenberg number is near the critical value.

"WINE GLASS STEM" PRESSURE DROP

The pressure drop in the naturally converging or wine glass stem funnel at the capillary entrance is not necessarily negligible. The results of this analysis can be used to estimate the magnitude of this loss. From Equations (5), (12), and (14) we have

$$\frac{\partial p(x,0)}{\partial x} = \frac{\alpha k_3}{(k_1 x + k_2)^3}$$

Integrating between 0 and L (the length of the wine glass stem) gives the center line pressure drop in two-dimensional flow as

$$\Delta p_{\mathbb{C}} = 2\alpha \frac{k_3}{k_1}\left[\frac{1}{k_2^2} - \frac{1}{(k_1 L + k_2)^2}\right] \tag{26}$$

As L approaches $-k_2/k_1$ (k_1 is a negative number) the center line pressure drop becomes infinitely large. Thus we have a consistent mechanism which can be used to predict the extra pressure loss currently accounted for by Bagley's (*6*) empirical end correction factor.

ACKNOWLEDGMENT

Aspects of this work have been discussed with Professor A. B. Metzner, Professor Gianni Astarita, and Professor J. C. Slattery whose comments are greatly appreciated. This study has been supported in part by the National Science Foundation.

NOTATION

f = integration function
F = similarity function
g = wall suction or injection parameter
$H = F/\alpha$
L = characteristic length
n = shear stress power law exponent
N = power law Reynolds number in s
N_{Deb} = Deborah number $= \lambda/t_p$
N_{Re} = power law Reynolds number in n
N_{WS} = Weissenberg number
p = pressure
R = wall profile
s = normal stress power law exponent
T_{ij} = deviatoric stress physical component
t_p = characteristic process time
u = axial velocity
U = characteristic axial velocity
v = transverse velocity
x = axial coordinate
y = transverse coordinate

Greek Letters

$\alpha = -N_{Re} R^3 f(x)/g$
δ = small number $\ll 1$
$\eta = y/R(x)$ similarity parameter
θ = channel half-angle
λ = characteristic time of the fluid
μ = apparent viscosity
ξ = normal stress coefficient
ρ = density
Ψ = stream function

LITERATURE CITED

1. Acrivos, Andrew, M. J. Shah, and E. E. Petersen, *Chem. Eng. Sci.*, **20**, 101 (1965).
2. Astarita, Gianni, *Ind. Eng. Chem. Fundamentals*, **6**, 257 (1967).
3. ———, *Ing. Chim. Ital.*, **2**, 74 (1966).
4. ———, *Can. J. Chem. Eng.*, **44**, 59 (1966).
5. ———, *Ind. Eng. Chem. Fundamentals*, **4**, 354 (1965).
6. Bagley, E. B., *J. Appl. Phys.*, **28**, 624 (1957).
7. ———, and A. M. Birks, *ibid.*, **31**, 556 (1960).
8. Balmer, R. T., D.Sc. dissertation, Univ. Virginia (1968).
9. Benbow, J. J., R. V. Charley, and P. Lamb, *Nature*, **192**, 223 (1961).
10. Berman, A. S., *J. Appl. Phys.*, **27**, 1557 (1956).

11. *Ibid.*, **24**, 1232 (1953).
12. Bird, R. B., W. E. Stewart, and E. N. Lightfoot, "Transport Phenomena," p. 14, Wiley, New York (1960).
13. Bizzell, G. D., and J. C. Slattery, *Chem. Eng. Sci.*, **17**, 777 (1962).
14. Blasius, H., *Z. Math. Phys.*, **58**, 225 (1910).
15. Clegg, P. L., in "The Rheology of Elastomers," Pergamon Press, New York (1958).
16. Collins, Morton, and W. R. Schowalter, *AIChE J.*, **9**, 98 (1963).
17. *Ibid.*, 804 (1963).
18. Drexler, L. H., M.Sc. thesis, Univ. Delaware, Newark (1967).
19. Gutfinger, Chaim, and Reuel Shinnar, *AIChE J.*, **10**, 631 (1964).
20. Hamel, G., *Jabresber. Dt. Mathematiker-Vereinigung*, **34**, (1916).
21. Hansen, A. G., "Similarity Analysis of Boundary Value Problems in Engineering," Prentice-Hall, Englewood Cliffs, N. J. (1964).
22. Hayasi, Nisiki, *J. Fluid Mech.*, 23, 293 (1965).
23. Hershey, H. C., and J. L. Zakin, *Ind. Eng. Chem. Fundamentals*, **6**, 381 (1967).
24. Jeffery, G. B., *Phil. Mag.*, **29**, 455 (1915).
25. Lee, S. Y., and W. F. Ames, *AIChE J.*, **12**, 700 (1966).
26. Metzner, A. B., *Ind. Eng. Chem.*, **50**, 1577 (1958).
27. ———, and Gianni Astarita, *AIChE J.*, 13, 550 (1967).
28. Metzner, A. B., J. L. White, and M. M. Denn, *ibid.*, **12**, 863 (1966).
29. ———, *Chem. Eng. Progr.*, **62**, 81 (1966).
30. Metzner, A. B., and J. L. White, *AIChE J.*, **11**, 989 (1965).
31. Metzner, A. B., W. T. Houghton, R. E. Hurd, and C. C. Wolfe, "Second Order Effects in Elasticity, Plasticity and Fluid Dynamics," p. 650, Pergamon Press, New York (1964).
32. Metzner, A. B., E. L. Carley, and I. K. Park, *Modern Plastics*, **37**, 133 (1960).
33. Millsaps, K. T., and Karl Pohlhausen, *J. Aero. Sci.*, 20, 187 (1953).
34. Mishra, S. P., and J. S. Roy, *Phys. Fluids*, 11, 2074 (1968).
35. Na, T. Y., and A. G. Hansen, *ASME Paper No. 67-WA/FE-2 (J. Basic Eng.)*.
36. Pearson, J. R. A., and C. J. S. Petrie, *Proc. 4th Intern. Rheol. Congr.*, **3**, 265 (1965).
37. Pohlhausen, Karl, *ZAMM*, **18**, 77 (1938).
38. Rosenhead, Louis, *Proc. Roy. Soc. London*, **175**, 436 (1940).
39. Savins, J. G., *Soc. Petrol. Eng. J.*, **4**, 203 (1964).
40. Schlichting, Hermann, "Boundary Layer Theory," 4th edit., McGraw-Hill, New York (1960).
41. Schowalter, W. R., *AIChE J.*, **6**, 24 (1960).
42. Sellars, J. R., *J. Appl. Phys.*, **26**, 489 (1955).
43. Seyer, F. A., and A. B. Metzner, *Can. J. Chem. Eng.*, **45**, 121 (1967).
44. Slattery, J. C., *AIChE J.*, **14**, 516 (1968).
45. Smith, D. K., Ph.D. dissertation, North Carolina State Univ., Raleigh (1965).
46. Spencer, R. S., and J. E. Dillon, *J. Colloid Sci.*, **4**, 241 (1949).
47. Tordella, J. P., *J. Appl. Polymer Sci.*, **7**, 215 (1963).
48. ———, *Rheol. Acta*, **1**, 216 (1958).
49. ———, *Trans. Soc. Rheo.*, **1**, 203 (1957).
50. ———, *J. Appl. Phys.*, **27**, 454 (1956).
51. Uebler, E. A., Ph.D. dissertation, Univ. Delaware, Newark (1966).
52. Weissenberg, Karl, "Proceedings of the First International Rheology Congress," pp. 1, 29, Scheveningen (1949).
53. White, J. L., *J. Appl. Polymer Sci.*, **8**, 2339 (1964).
54. ———, and N. J. Tokita, *ibid.*, **10**, 1011 (1966).
55. White, J. L., and A. B. Metzner, *AIChE J.*, **11**, 324 (1965).
56. Williams, J. C. III, *AIAA J.*, **1**, 186 (1963).
57. ———, *USCEC Rept. 83-213* (June 1962).
58. Yuan, S. W., *J. Appl. Phys.*, **27**, 267 (1956).

Manuscript received October 8, 1968; revision received July 28, 1969; paper accepted July 31, 1969.

Polymerization in Expanding Catalyst Particles

W. R. SCHMEAL and J. R. STREET[a]

Shell Development Company, Emeryville, California

Four models are presented to describe polymerization in expanding catalyst particles. The globules are presumed to be expanding with accumulating polymer, and catalytic reaction sites are dispersed throughout the polymer matrix which is forming about them. Monomer must diffuse through the polymer to polymerize at the catalyst sites.

The Thiele modulus (α), $R\sqrt{kl/D}$, is a ratio of characteristic diffusion time to reaction time which is a measure of the importance of diffusion relative to reaction. Polymerization rates are predicted by the models which are generally dependent on the controlling mechanism. Broad molecular weight distributions are predicted for cases of diffusion control (large α) for those models in which catalyst sites are not equally accessible to monomer.

Polymerization rates decline toward an asymptotic final value as the particles expand in diffusion-controlled cases. Most of the decline which would be readily observable in a laboratory experiment would have occurred by the time the particle radii had increased to about three times their original value.

Solid polymerization catalysts fluidized in a material that does not dissolve the polymer expand with accumulating polymer during reaction. These particles may grow more than 10,000-fold in volume during polymerization. In fact, since catalysts are generally much more expensive per unit weight than the polymers they produce, a considerable increase in size during polymerization is usually a prerequisite for the associated process to have commercial value. Otherwise, the catalyst must be recovered.

[a]Present address, Shell Chemical Company, Deer Park, Texas.